Dalton Transactions

RSCPublishing

COMMUNICATION

View Article Online
View Journal | View Issue

Cite this: *Dalton Trans.*, 2013, **42**, 6701

Received 15th February 2013,
Accepted 21st March 2013

DOI: 10.1039/c3dt50429h

www.rsc.org/dalton

Stepwise replacement of nickel with cobalt ions in a [Ni_6] cluster†

Graham N. Newton, Hiroki Sato, Takuya Shiga and Hiroki Oshio*

Polydentate ligands were used to support planar methoxo-bridged {$Ni_{6-x}Co_x$} (x = 0, 1 or 2) clusters which were structurally characterized by single crystal analyses. The homometallic {Ni_6} complex displayed overall ferrimagnetic interactions between metal centres, and increasing the cobalt content led to a proportional increase in ac-response.

The synthesis of novel polynuclear transition metal complexes continues to attract a great deal of research interest due to the propensity of such clusters to display remarkable physical characteristics such as multi-redox activity,[1] single molecule magnet (SMM) behaviour[2] and magnetic bistability.[3] Complexes in which metal ions are bridged by oxygen-donor ligands to form cubane or open-cubane arrangements have been widely reported and are promising systems for the study of molecular magnetism,[4] and as mimics of biological systems.[5] Neighbouring metal ions in such complexes are usually bridged by oxygen donor ligands at angles close to 90°, leading to accidental orthogonality of the interacting magnetic orbitals and ferromagnetic interactions.[6] Planar multidentate ligands are good candidates for the semi-directed synthesis of multinuclear magnetic clusters due to their propensity to form regular, close-knit metal ion arrays, such as grids, rings and squares.[7] The use of planar alkoxo/phenoxo donors may allow the synthesis of extended clusters with open-cubane framework structures and ferromagnetic ground states, and is therefore a promising approach towards the synthesis of new polynuclear clusters with high spin ground states. In this study we synthesized a planar {Ni_6} complex with an open-cubane type framework and investigated the effect of the incorporation of heterometal ions on the magnetic properties.

The multidentate planar ligand 1,3-bis-(2-hydroxyphenyl)-1,3-propanedione (H_3L) was synthesized by the Claisen condensation of 2-hydroxyacetophenone and ethyl salicylate, following a slightly modified version of the previously reported method (Scheme S1†).[8] Combination with $NiCl_2·6H_2O$ and triethylamine in methanol allowed the isolation of yellow crystals of $[Ni_6(HL)_4(MeO)_4(MeOH)_6]·4MeOH$ (**1**·4MeOH),‡ a complex of higher nuclearity than those previously reported with H_3L.[8]

The cluster contains a hexanuclear nickel core similar to those of complexes reported by Tandon *et al.*,[9] and McInnes and co-workers,[10] in which the nickel ions are bridged by four μ_3-methoxo ligands and supported by the β-diketone (central) and ketone/phenoxide (outer) binding sites of four dianionic ligands (HL^{2-}). The deprotonation state of the ligands was predicted from charge balance and their bonding behaviour. **1** crystallises in the monoclinic space group $P2_1/n$, and the asymmetric unit contains three nickel centres. All three metal ions have subtly different distorted octahedral O_6 coordination environments. Ni1 is coordinated by one central and one outer bidentate binding site from two HL^{2-} ligands, and its coordination sphere is completed by the coordination of two μ_3-methoxo groups. Ni2 is bound by one outer HL^{2-} bidentate site, three μ_3-methoxo ligands and one methanol molecule, and Ni3 is chelated by the central site of one HL^{2-} ligand, one μ_3-methoxo moieties and two solvent methanol molecules.

The contrasting coordination environments lead to subtle differences in the average Ni–O bonding distances of 2.031(6), 2.039(6) and 2.065(7) Å for Ni1, Ni2 and Ni3, respectively, while all show substantial distortion from ideal octahedral geometry (Table S1†). It is interesting to note that the distortion of the coordination geometry of Ni3 results in the elongation of the bonds along one axis with Ni3–O8 and Ni3–O11 bond lengths of 2.135(6) and 2.115(6) Å, respectively (Fig. 1).

The difference in the coordination environments of the three metal centres, as shown by the X-ray analysis, prompted our attempts to generate heterometallic derivatives, and conducting the corresponding syntheses using Ni : Co ratios of

---

Department of Chemistry, Graduate School of Pure and Applied Sciences, University of Tsukuba, Tennodai 1-1-1, Tsukuba 305-8571, Japan.
E-mail: oshio@chem.tsukuba.ac.jp; Fax: +81 29 853 4238; Tel: +81 29 853 4238

† Electronic supplementary information (ESI) available: Additional experimental, magnetic and structural data and three cif files. CCDC 924183–924185. For ESI and crystallographic data in CIF or other electronic format see DOI: 10.1039/c3dt50429h

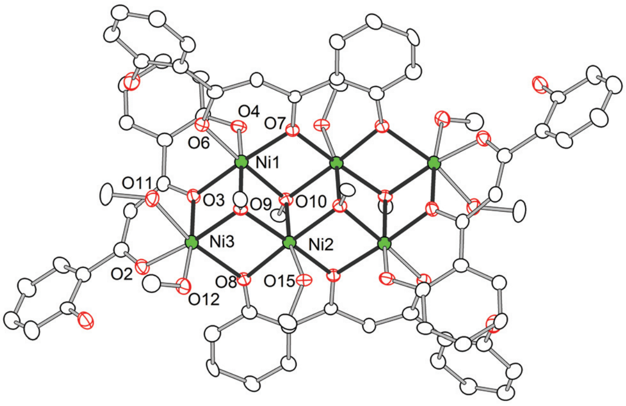

Fig. 1 The crystallographically determined structure of **1**, viewed perpendicular to the plane of the metal ions. Nickel ions are in green, and oxygen and carbon atoms in red and white, respectively. Thermal ellipsoids are shown at 30% probability, and lattice solvent molecules and hydrogen atoms have been removed for clarity.

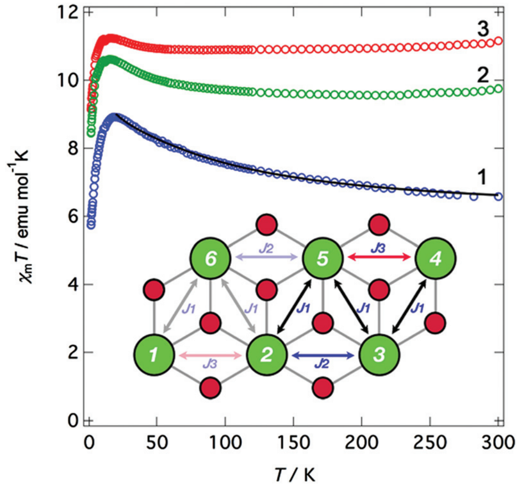

Fig. 2 Magnetic susceptibility data for **1** (blue), **2** (green) and **3** (red), with the fitting data for **1** in black. Inset: magnetic exchange pathways in **1**, weak ferromagnetic in black, strong ferromagnetic in blue and antiferromagnetic in red.

Table 1 Interatomic distances and Ni–O–Ni bridging angles for complex **1**

M···M	Dist. (Å)	M–O–M	Ang. (°)	J
Ni2′–Ni2	3.09	Ni2′–O10–Ni2	97.61	J_1 = +1.7 K
Ni1–Ni2′	3.01	Ni1–O7–Ni2′	95.81	J_2 = +35.5 K
		Ni1–O10–Ni2′	96.82	
Ni1–Ni2	3.05	Ni1–O10–Ni2	96.40	J_1 = +1.7 K
		Ni1–O9–Ni2	95.84	
Ni2′–Ni3	3.08	Ni2′–O8–Ni3	96.48	J_3 = −2.5 K
		Ni2′–O9–Ni3	99.52	
Ni1–Ni3	3.06	Ni1–O3–Ni3	97.75	J_1 = +1.7 K
		Ni1–O9–Ni3	95.89	

5 : 1 and 4 : 2 led to the isolation of $[Ni_5Co(HL)_4(MeO)_4(MeOH)_6]\cdot4MeOH$ (**2**·4MeOH) and $[Ni_4Co_2(HL)_4(MeO)_4(MeOH)_6]\cdot4MeOH$ (**3**·4MeOH), respectively. Compounds **2** and **3** are isostructural to **1**, with divalent cobalt ions replacing one and two nickel centres, respectively. Elemental and ICP analyses confirmed the chemical composition of the clusters and the single crystal analysis on **2** and **3** permitted the identification of the cobalt centres. In both complexes, the cobalt ions appeared to be located in the positions equivalent to the Ni3 positions of complex **1**, with cobalt and nickel ions substitutionally disordered between the two equivalent sites in **2**, and cobalt occupying both in **3**. The average M–O bond distances were 2.028(3), 2.040(2) and 2.084(5) Å for Ni1, Ni2 and Ni3/Co1, respectively in complex **2**, and 2.035(3), 2.045(3) and 2.096(3) Å for Ni1, Ni2 and Co1 respectively in **3** (Table S1†); significantly different only in the Co1/Ni3 position.

Magnetic susceptibility measurements were conducted for compounds **1**, **2** and **3** over a temperature range of 300–1.8 K under a magnetic field of 0.05 T (Fig. 2 and S1†). Compound **1** had a $\chi_m T$ value of 6.58 emu mol^{-1} K at 300 K, slightly greater than the value expected for the uncorrelated spins of six nickel ions (6.0 emu mol^{-1} K, g = 2.0). As the measurement temperature was lowered, the $\chi_m T$ value increased slowly to reach a maximum of 8.93 emu mol^{-1} K at 19 K, before decreasing to reach a final value of 5.74 emu mol^{-1} K at 1.8 K. The low temperature maximum was much less than 21 emu mol^{-1} K, the value expected for six ferromagnetically coupled nickel centres (g = 2.0), suggestive of a ferrimagnetic ground state. The bonding distances and angles permitted the identification of three independent magnetic coupling pathways within the cluster core (Fig. 2, inset),[9] and the data were analysed using the following spin Hamiltonian:

$$\hat{H} = -2\{(J_1(\hat{S}_2\hat{S}_5) + J_2(\hat{S}_2\hat{S}_3) + J_2(\hat{S}_5\hat{S}_6) + J_1(\hat{S}_3\hat{S}_5) + J_1(\hat{S}_2\hat{S}_6) + J_3(\hat{S}_1\hat{S}_2) + J_3(\hat{S}_4\hat{S}_5) + J_1(\hat{S}_1\hat{S}_6) + J_1(\hat{S}_3\hat{S}_4)\}$$

using MAGPACK,[11] to yield fitting parameters of g = 2.00, J_1 = +1.7 K, J_2 = +35.5 K and J_3 = −2.5 K. The obtained J values suggest that both ferro- and antiferromagnetic pathways are operative in complex **1**, and the bridging angles and intermetallic distances offer evidence in support of the fitted parameters (Table 1). Ni–O–Ni angles of around 90° (below 98–99°) are known to mediate ferromagnetic coupling pathways,[6] and thus the bonding angles suggest that J_1 and J_2 are ferromagnetic, and that the large Ni2–O–Ni3 bridging angles (av. = 98.0°) may result in an antiferromagnetic pathway (J_3). The small Ni1–O–Ni2 bridging angles (av. = 96.3°) coupled with the short interatomic distance (3.01 Å) suggest that J_2 may be a strongly ferromagnetic pathway.

The sudden decrease in the susceptibility data at low temperature can be ascribed to a combination of zero-field splitting and intermolecular effects.[9] The clusters adopt a columnar packing arrangement, with a shortest Ni···Ni distance of *ca.* 7.5 Å between the complex moieties. Methanol molecules form hydrogen-bonded bridges between neighbouring columns but the long distance between metal ions (*ca.* 10.8 Å) suggests that the strongest intermolecular magnetic pathway is likely to be intracolumnar (Fig. S2†). Reduced magnetization measurements, conducted to estimate the complex D value, were unsuccessful due to the partial population of low-lying states close to the ground state.

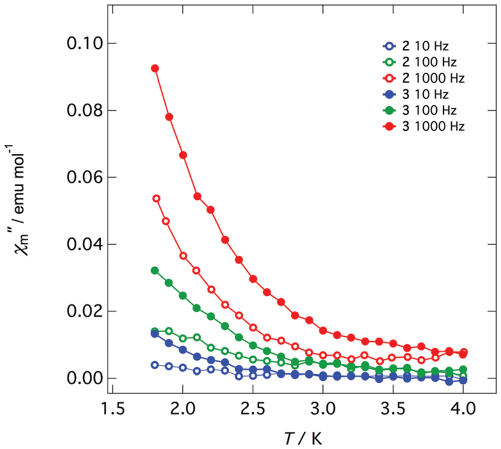

Fig. 3 Out-of-phase ac susceptibility data for complexes **2** (empty circles) and **3** (filled circles), measured at 10 (blue), 100 (green) and 1000 Hz (red) at 1.8–4.0 K.

Magnetic susceptibility measurements were conducted on **2** and **3** under the same conditions as **1**. **2** and **3** had $\chi_m T$ values of 9.76 and 11.16 emu mol^{-1} K respectively at 300 K, values that initially decreased slightly as the temperature was lowered until they began to increase at approximately 80 and 50 K, reaching maxima of 10.62 and 11.24 emu mol^{-1} K at 16 and 15 K before rapidly decreasing to 8.45 and 9.16 emu mol^{-1} K respectively at 1.8 K. The susceptibility plots of **2** and **3** differ in profile from that of **1**, due to the orbital contribution associated with Co^{II} ions; the relatively small increases in $\chi_m T$ at low temperatures suggest that both show ferrimagnetic behaviour. The magnetization plots for **1**, **2** and **3** are shown in Fig. S3.†

Ac magnetic susceptibility measurements were conducted on all three samples. Complex **1** showed no ac response, but the data collected for complexes **2** and **3** indicated the occurrence of slow magnetic relaxation (Fig. 3). The scale of the magnetic response appeared to be proportional to the cluster cobalt content. The existence of an easy axis of magnetization may be understood by considering the distorted coordination geometry of the cobalt binding sites. In **2** and **3** the Co ions each have one elongated axis with Co1–O8/Co1–O11 bond distances of 2.159(4)/2.176(5) and 2.174(3)/2.198(3) Å, respectively. The two bond vectors run approximately parallel to the length of the cluster (Fig. S4†). The inclusion of one Co ion in **2** leads to a very small ac response, while the semi-alignment of the distortion axes in **3** amplifies the behaviour, probably through a combination of increasing the negative anisotropy and the number of spins. Despite the improved ac response, however, the energy barriers of magnetic relaxation could not be determined at 1.8 K.

Conclusions

Complexation of the planar multidentate ligand 1,3-bis-(2-hydroxyphenyl)-1,3-propanedione with nickel chloride led to the isolation of a hexanuclear {Ni$_6$} cluster in which the nickel ions existed in three distinct coordination environments. Subsequent syntheses performed using mixtures of nickel and cobalt chloride salts led to the generation of mono- and di-substituted heterometallic clusters, {Ni$_5$Co} and {Ni$_4$Co$_2$}. The composition of the heterometallic clusters was supported by X-ray crystallography, elemental analysis and magnetic susceptibility measurements. The magnetization data also showed that the inclusion of increasing numbers of cobalt ions led to improved frequency response. This observation is an example of the importance of the controlled generation of heterometallic clusters, in which physical properties can be tuned by altering the electronic and magnetic interactions between neighbouring metal centres.

Notes and references

‡[Ni$_6$(HL)$_4$(MeO)$_4$(MeOH)$_6$]·4MeOH (**1**·4MeOH): To a solution of H$_3$L (25 mg, 0.1 mmol) and triethylamine (56 μL, 0.4 mmol) in methanol (40 mL), a solution of NiCl$_2$·6H$_2$O (36 mg, 0.151 mmol) in methanol (5 mL) was added dropwise. The dark yellow solution was stirred at room temperature for 10 minutes, and left untouched for crystallization by slow evaporation. After 2 days dark yellow needle crystals of **1**·4MeOH were collected by filtration (12 mg, 0.0066 mmol, 26.5%) and dried. Elemental analysis calcd for (**1**·3.5H$_2$O), C$_{70}$H$_{83}$Ni$_6$O$_{29.5}$: C, 48.08; H, 4.78. Found: C, 47.74; H, 4.48. [Ni$_5$Co(HL)$_4$(MeO)$_4$(MeOH)$_6$]·4MeOH (**2**·4MeOH): To a solution of H$_3$L (25 mg, 0.1 mmol) and triethylamine (56 μL, 0.4 mmol) in methanol (40 mL), a solution of NiCl$_2$·6H$_2$O (30 mg, 0.126 mmol) and CoCl$_2$·4H$_2$O (6 mg, 0.025 mmol) in methanol (5 mL) was added dropwise. The orange solution was stirred at room temperature for 10 minutes before being left untouched for crystallization by slow evaporation. After 2 days light brown needle crystals of **2**·4MeOH were collected by filtration and dried (10.88 mg, 0.006 mmol, 24.0%). Elemental analysis calcd for (**2**·3H$_2$O), C$_{70}$H$_{82}$CoNi$_5$O$_{29}$: C, 48.33; H, 4.75. Found: C, 48.05; H, 4.62. ICP calcd Ni: 5.00; Co: 1.00. Found: Ni: 5.56; Co: 1.0. [Ni$_4$Co$_2$(HL)$_4$(MeO)$_4$(MeOH)$_6$]·4MeOH (**3**·4MeOH): To a solution of H$_3$L (25 mg, 0.1 mmol) and triethylamine (56 μL, 0.4 mmol) in methanol (40 mL), a solution of NiCl$_2$·6H$_2$O (24 mg, 0.100 mmol) and CoCl$_2$·4H$_2$O (12 mg, 0.051 mmol) in methanol (5 mL) was added dropwise. The orange-brown solution was stirred at room temperature for 10 minutes, before being left untouched for crystallization by slow evaporation. After 2 days orange-brown needle crystals of **3**·4MeOH were collected by filtration and dried (11.85 mg, 0.0065 mmol, 26.1%). Elemental analysis calcd for (**3**·3H$_2$O), C$_{70}$H$_{82}$Co$_2$Ni$_4$O$_{29}$: C, 48.32; H, 4.75. Found: C, 48.03; H, 4.25. ICP calcd Ni: 2.00; Co: 1.00. Found: Ni: 2.23; Co: 1.0. Crystallographic data for **1**·4MeOH: [C$_{70}$H$_{76}$Ni$_6$O$_{26}$]·4MeOH, M_r = 1813.74, monoclinic, $P2_1/n$, a = 8.578(6) Å, b = 27.265(19) Å, c = 15.964(11) Å, β = 94.540(13)°, V = 3722(4) Å^3, Z = 2, T = 100 K. A total of 18 414 reflections were collected (2.96° < 2θ < 50.25°) of which 6638 unique reflections (R_{int} = 0.1019) were measured. R_1 = 0.0706, wR_2 = 0.1694 ($I > 2\sigma(I)$). **2**·4MeOH: [C$_{70}$H$_{76}$CoNi$_5$O$_{26}$]·4MeOH, M_r = 1813.96, monoclinic, $P2_1/n$, a = 8.5016(7) Å, b = 27.218(2) Å, c = 16.0744(12) Å, β = 94.700(2)°, V = 3707.0(5) Å^3, Z = 2, T = 100 K. A total of 19 910 reflections were collected (2.94° < 2θ < 50.50°) of which 6901 unique reflections (R_{int} = 0.0294) were measured. R_1 = 0.0495, wR_2 = 0.1289 ($I > 2\sigma(I)$). **3**·4MeOH: [C$_{70}$H$_{76}$CoNi$_5$O$_{26}$]·4MeOH, M_r = 1814.18, monoclinic, $P2_1/n$, a = 8.4933(11) Å, b = 27.255(3) Å, c = 16.116(2) Å, β = 94.750(2)°, V = 3717.7(8) Å^3, Z = 2, T = 100 K. A total of 20 037 reflections were collected (2.94° < 2θ < 50.50°) of which 6917 unique reflections (R_{int} = 0.0409) were measured. R_1 = 0.0564, wR_2 = 0.1377 ($I > 2\sigma(I)$).

1 (*a*) V. Balzani, A. Juris, M. Venturi, S. Campagna and S. Serroni, *Chem. Rev.*, 1996, **96**, 759; (*b*) T. Ito, T. Hamaguchi, H. Nagino, T. Yamaguchi, J. Washington and C. P. Kubiak, *Science*, 1997, **277**, 660.

2 *Molecular Nanomagnets*, ed. D. Gatteschi, R. Sessoli and J. Villain, Oxford Press, New York, 2006.

3 M. Nihei, Y. Sekine, N. Suganami, K. Nakazawa, A. Nakao, H. Nakao, Y. Murakami and H. Oshio, *J. Am. Chem. Soc.*, 2011, **133**, 3592.

4 K. Isobe and A. Yagasaki, *Acc. Chem. Res.*, 1993, **26**, 524.

5 G. C. Dismukes, R. Brimblecombe, G. A. N. Felton, R. S. Pryadun, J. E. Sheats, L. Spiccia and G. F. Swiegers, *Acc. Chem. Res.*, 2009, **42**, 1935.

6 (*a*) M. A. Halcrow, J. S. Sun, J. C. Huffman and G. Christou, *Inorg. Chem.*, 1995, **34**, 4167; (*b*) J. M. ClementeJuan, B. Chansou, B. Donnadieu and J. P. Tuchages, *Inorg. Chem.*, 2000, **39**, 5515; (*c*) P. Mukherjee, M. G. B. Drew, C. J. Gómez-García and A. Ghosh, *Inorg. Chem.*, 2009, **48**, 5848; (*d*) F. Iijima, K. Hasumi, T. Shiga, G. N. Newton and H. Oshio, *Chem. Lett.*, 2012, 691.

7 (*a*) T. Shiga, T. Matsumoto, M. Noguchi, T. Onuki, N. Hoshino, G. N. Newton, M. Nakano and H. Oshio, *Chem.–Asian J.*, 2009, **4**, 1660; (*b*) G. N. Newton, T. Onuki, T. Shiga, M. Noguchi, T. Matsumoto, J. S. Mathieson, M. Nihei, M. Nakano, L. Cronin and H. Oshio, *Angew. Chem., Int. Ed.*, 2011, **50**, 4844; (*c*) T. Matsumoto, T. Shiga, M. Noguchi, T. Onuki, G. N. Newton, N. Hoshino, M. Nakano and H. Oshio, *Inorg. Chem.*, 2010, **49**, 368; (*d*) G. N. Newton, T. Shiga and H. Oshio, *Sci. China Chem.*, 2012, **55**, 973.

8 (*a*) F. Eiden and H. D. Shweiger, *Synthesis*, 1974, 511; (*b*) F. Teixidor, A. Llobet, L. Eschriche and J. Casabó, *Polyhedron*, 1985, **4**, 215; (*c*) F. Teixidor, J. Colomer, J. Casabó, J. Ruis, E. Molins and C. Miravitles, *Inorg. Chem.*, 1989, **28**, 678.

9 S. S. Tandon, S. D. Bunge, J. Sanchiz and L. K. Thompson, *Inorg. Chem.*, 2012, **51**, 3270.

10 R. T. W. Scott, L. F. Jones, I. S. Tidmarsh, B. Breeze, R. H. Laye, J. Wolowska, D. J. Stone, A. Collins, S. Parsons, W. Wernsdorfer, G. Aromí, E. J. L. McInnes and E. K. Brechin, *Chem.–Eur. J.*, 2009, **15**, 12389.

11 J. J. Borrás-Almenar, J. M. Clemente-Juan, E. Coronado and B. S. Tsukerblat, *J. Comput. Chem.*, 2001, **22**, 985.